Supplemental Informations

1. Supplemental figures

Figure S1, **Binding domains of OPHN1 with its partners.**

A) Mapping of the Proline-rich regions of OPHN1 involved in the binding to CIN85 (ABC), Amphiphysin (AmphiI and II) and endophilin (EENB1 and 2). Amphiphysin and CIN85 have overlapping binding sites to OPHN1 CterA whereas endophilins binds the OPHN1 CterB **B)** Mapping of the SH3 domains of CIN85 involved in the binding to OPHN1. The SH3 B site alone is able to bind to OPHN1 and adding either the A site or the C site increases the affinity to Cter A. SM: Starting material; CS: Coomassie Staining of SDS-PAGE gels is presented as loading controls.

FigureS2, **Loss of ophn1 function activates RhoA/ROCK pathway and reduces the transferrin Receptor endocytosis.**

A) Activation of RhoA in *Ophn1*$^{+/y}$ and *Ophn1*$^{-/y}$ fibroblasts cells in response to five minutes of serum stimulation were measured by GST-Rhotekin binding domain pull-down assay. *Ophn1*$^{-/y}$ cells presents x1.8 more activation than *Ophn1*$^{+/y}$ as estimated from the ratio GTP bound RhoA (active) to the total amount of RhoA proteins (total).

B) Cultured astroglial cells from *Ophn1*$^{-/y}$ showed an increase (x1.4) of phosphorylation of MYPT1, one of ROCK substrate. Inhibition of ROCK by 10 µM Fasudil (HA1077) for 2 hours abolishes the phosphorylation of MYPT1 in both genotypes.

C) Transferrin receptor internalization assays using fluorecent labelled transferrin and FACS analyses in *Ophn1*$^{+/y}$ and *Ophn1*$^{-/y}$ astroglial cells pre-treated (+) or not (-) with 10µM Rho-kinase inhibitor Y27632. *Ophn1*$^{-/y}$ cells showed 64% decrease compared to *Ophn1*$^{+/y}$ (*Ophn1*$^{+/y}$: 87 ± 11; *Ophn1*$^{-/y}$: 31 ± 4; two-tailed Students t-test $p<0.01$,n=4). Treatment of *Ophn1*$^{-/y}$ cells with 10µM Y27632 prior to transferrin uptake rescues the level of endocytosis to *Ophn1*$^{+/y}$.

FigureS3, **Internalization assays of AMPAR GLUR1 and GLUR2 sub-units in neuronal cell culture.**

Percentages of receptor internalization, as defined in Material and Method section, was determined at different time points for both genotype and compared using Student t-test. Only GLUR1 internalization was impaired by OPHN1 loss of function.

FigureS4, **NMDA-dependent Long Term Depression (LTD) at the CA3:CA1 synapse in ophn1+/y hippocampal slices.**

Ai and Aii, Addition of 10µM Y27632 to *Ophn1*$^{+/y}$ slices before and during the LTD protocol did not alter the PSP amplitude showing the specificity of LTD rescue in ophn1$^{-/y}$. Bi and Bii, Treatment of ophn1$^{+/y}$ slices with NMDA inhibitor, D-APV, abolished the LTD induced by repetitive stimulation at low frequency.

FigureS5, **Schematic illustration of the OPHN1/RhoA/ROCK/endophilin pathway involved in clathrin-mediated endocytosis**.

Under normal physiological conditions (black arrows, physiology), OPHN1 is localized on both pre- and postsynaptic compartments. With its proline-rich sites in the C-terminal domain, OPHN1 interacts with the SH3 containing proteins: endophilins, amphyphisins and CIN85, all three proteins are involved in clathrin-mediated endocytosis (CME). These interactions would be able to remove the inhibition effect of the N-terminal domain of OPHN1 on its central RhoGAP domain (Fauchereau et al, 2003) resulting locally in the down-regulation of RhoA and its effector ROCK, finally helping CME.

Loss of OPHN1 function (red cross, pathology) leads to the activation of RhoA/ROCK pathway (red Arrows up), reducing synaptic vesicle endocytosis and AMPA receptor recycling (red arrow down). *In vitro* treatment with ROCK inhibitor Y27632 (in blue, therapy) rescues the CME deficit and synaptic plasticity in *Ophn1*$^{-/y}$ model. Studies from Kaneko et al. (Kaneko et al, 2005) provide the direct link from ROCK activation to endocytosis through the control of endophilin phosphorylation and its interaction with CIN85. Alternatively, ROCK could modulate the phosphorylation of other substrates as the Myosin Light Chain Kinase to control the acto-myosin contractility around the endocytic sites.

Khelfaoui_ Fig. S1.

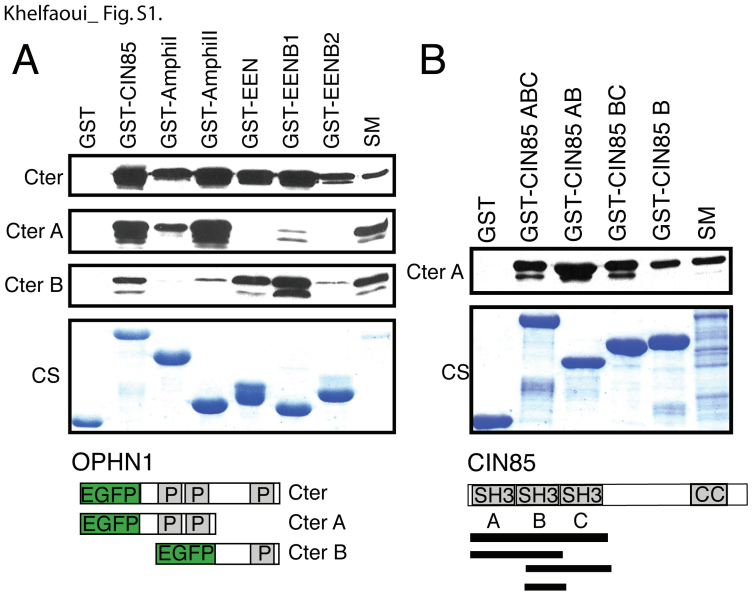

Khelfaoui_ Fig. S2.

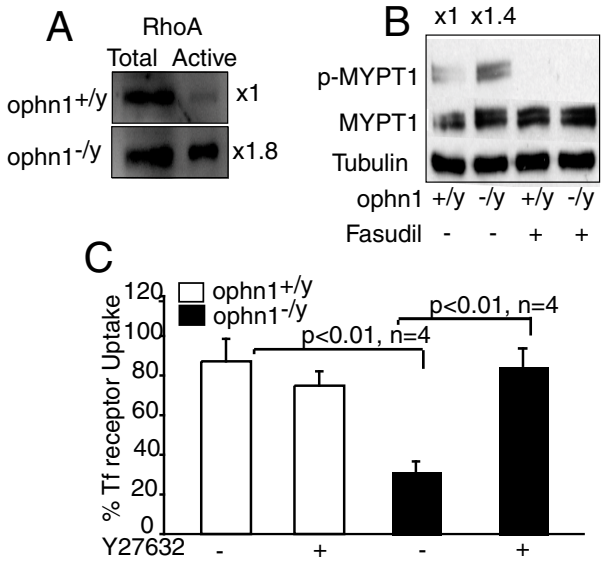

Khelfaoui_ Fig. S3.

Time (min)	**5**		**10**		**15**		**20**	
Genotype	ophn1$^{+/y}$	ophn1$^{-/y}$	ophn1$^{+/y}$	ophn1$^{-/y}$	ophn1$^{+/y}$	ophn1$^{-/y}$	ophn1$^{+/y}$	ophn1$^{-/y}$
GLUR1								
mean (%)	82	66	80.7	61.5	76	59.4	70	61.8
SE	3	2.8	5.5	4.1	4.6	5.4	3.3	6.6
p (t test)	≤ 0.001		≤ 0.001		≤ 0.001		≤ 0.001	
GLUR2								
mean (%)	66	69	69	73	78	80	70	71
SE	5.5	3	5.3	4	3.8	6	1.8	7.8
p (t test)	0.45		0.09		0.45		0.95	

Figure S3: Pourcentage of AMPA Receptor Internalisation in neuronal cell cultures from ophn1 $^{+/y}$ and ophn1$^{-/y}$ embryos.

Khelfaoui_ Fig. S4.

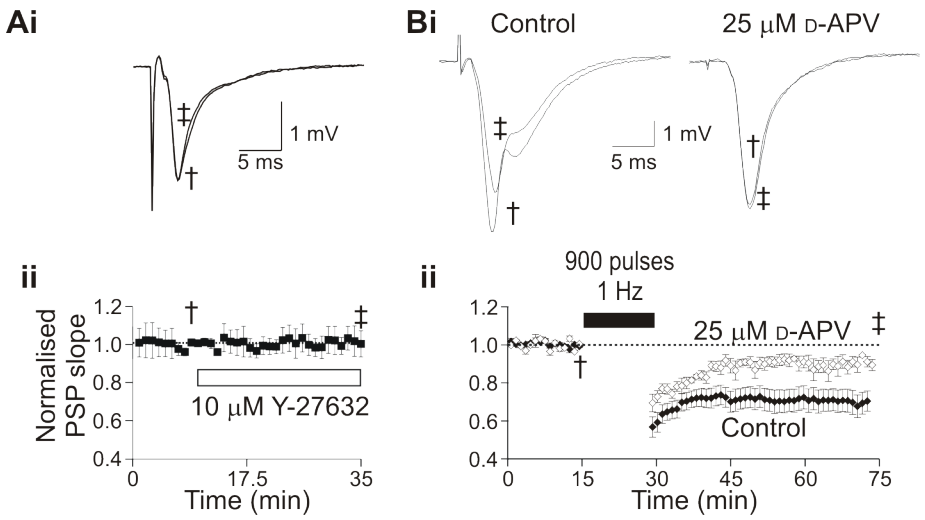

Khelfaoui_ Fig. S5.